

Research Report

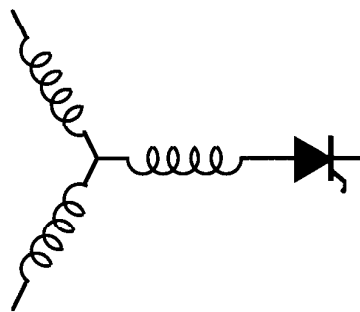
96-48

**Input Power Factor Control of AC-DC Series  
Resonant DC Link Converter Using PID Operation.**

**H. Soebagia\*, M. Yoshida\*, Y. Murai\*, T.A. Lipo**

Wisconsin Power Electronics  
Research Center  
University of Wisconsin-Madison  
Madison WI 53706-1691

\*Gifu University  
1-1 Yanagido  
Gifu 501-11  
Japan



**Wisconsin  
Electric  
Machines &  
Power  
Electronics  
Consortium**

University of Wisconsin-Madison  
College of Engineering  
Wisconsin Power Electronics Research Center  
2559D Engineering Hall  
1415 Engineering Drive  
Madison WI 53706-1691

# Input Power Factor Control of AC-DC Series Resonant DC Link Converter Using PID Operation

Hasto Soebagia, Masaharu Yoshida, Yoshihiro Murai, *Senior Member, IEEE*, and Thomas A. Lipo, *Fellow, IEEE*

**Abstract**—This paper proposes a method of power factor control for the three-phase input current of ac-dc series resonant dc link converter systems. The proposed system has fast response, using high frequency resonance, soft switching (zero current switching), and natural commutation of thyristor switches. By implementing the PID operation strategy for switching control, the system performs reliable operation in the input power factor control, and the elimination of higher harmonic components can be achieved dramatically. The numerical and experimental results are presented in this paper.

## I. INTRODUCTION

**M**ANY types of ac-dc converters are used extensively for electronics equipment in domestic, office, and factory automation applications. These ac-dc converters are well known to obtain adjustable dc voltage from an ac source.

Up to now, the ac-dc converter of the uncontrolled rectifier and line commutated phase-control have been dominant in many applications. The inherent drawback of these converters is that the power factor depends on the firing angle. When the firing angle increases, the power factor decreases and the line current contains a lot of harmonics.

These drawbacks have been improved in references [1]–[3]. Manias *et al.* [1] proposed a simple and novel switch-mode rectifier (SMR) structure that has six force-commutated switches with bidirectional current flow. Their method [1] makes the input power factor controllable by utilizing the PWM method. The method, however, still generates a lot of harmonics in the input current. Inagaki *et al.* [2] utilized the PWM control method for the SMR, based on the idea of coordinate transformation. In their method, the iron loss in the transformer may become visible because of high frequency. Wu *et al.* [3] manipulated the predicted current control strategy with fixed switching frequency to the PWM ac-to-dc converter. In those methods [1]–[3], the switching losses are fairly big because of the utilization of force commutation switches. Recently, a high frequency series resonant dc link power converter has been developed to obtain low switching losses, high power density, and fast response [4]–[6]. This converter is composed of a six thyristors bridge and has a simple configuration and

minimum number of devices, as well as high current and high voltage margins [7].

This paper proposes a method of the input power factor control of ac-dc series resonant dc link converter systems, as shown in Fig. 1. The switching control of the converter is very important to realize the input power factor control (unity or other power factor) and the elimination of high harmonic components [8], [9]. In the converter switching, the PID operation strategy is employed to make input current in phase or in desired phase angle with voltage source and to regulate the output dc current. The proposed converter characteristics are verified by computer simulation and experimental results.

## II. STRATEGY FOR INPUT POWER FACTOR CONTROL

### A. AC-DC Series Resonant DC Link Converter

As shown in Fig. 1, the ac-dc series resonant dc link converter is composed of a six thyristors bridge, input low pass filter  $L_f$  and  $C_f$ , resonant element  $L_0$  and  $C_0$ , bias inductance  $L_d$ , and load  $R_L$ . The resonant element generates resonant current pulses  $i_s$  in which the dc bias current  $I_d$  is superimposed on the resonant current by large inductance  $L_d$ . The switching of the thyristor is performed at zero current instant of resonant current to reduce switching losses. The low pass filter  $L_f$  and  $C_f$  are needed to maintain resonant current and to obtain better sinusoidal waveform of input line current. The following equations can be derived from Fig. 1:

$$-V_d + v_{C_0}(t) + L_0 \frac{di_s(t)}{dt} + v_L(t) = 0 \quad (1)$$

$$v_{C_0}(t) = L_d \frac{dI_d(t)}{dt} \quad (2)$$

$$C_0 \frac{dv_{C_0}(t)}{dt} = i_s(t) - I_d(t) \quad (3)$$

$$C_L \frac{dv_L(t)}{dt} = i_s(t) - \frac{v_L(t)}{R_L} \quad (4)$$

In general,  $L_d$  and  $C_L$  are sufficiently large to maintain the current  $I_d$  and the voltage  $v_L$  almost constant. Assume that two thyristors,  $T_a^+$  and  $T_c^-$ , for example, are switched to the conducting state at  $t = 0$ , as shown in Fig. 1. From the steady state solutions of these differential equations,  $i_s(t)$  and  $v_{C_0}(t)$  are given as follows:

$$i_s(t) = (V_{sw}/Z_0) \sin \omega_0 t + I_d(1 - \cos \omega_0 t) \quad (5)$$

$$v_{C_0}(t) = (V_d - V_L) - V_{sw} \cos \omega_0 t - Z_0 I_d \sin \omega_0 t \quad (6)$$

Manuscript received June 4, 1994; revised August 10, 1995.  
H. Soebagia, M. Yoshida, and Y. Murai are with Gifu University, Gifu, Japan.

T. A. Lipo is with the University of Wisconsin, Madison, WI 53706 USA.  
Publisher Item Identifier S 0885-8993(96)00594-7.

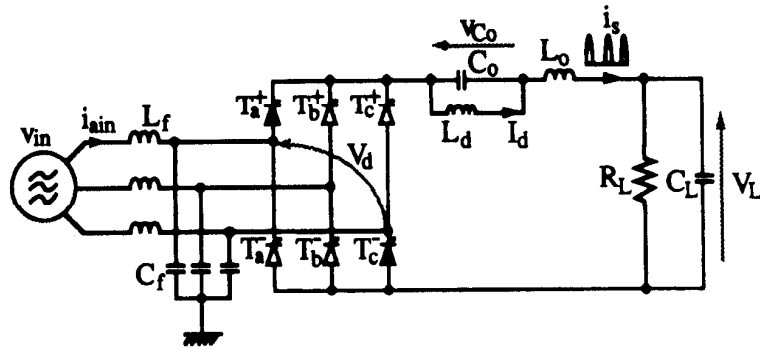


Fig. 1. Main circuit of series resonant dc link converter.

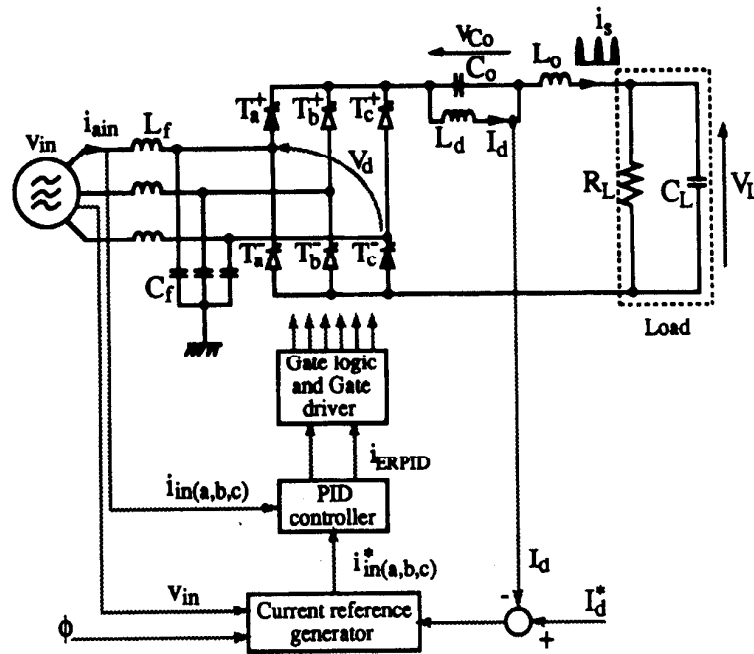


Fig. 2. Block diagram of control system.

where

$$\omega_0 = \frac{1}{\sqrt{L_0 C_0}}, \quad Z_0 = \sqrt{\frac{L_0}{C_0}}$$

$$V_{sw} = V_d - V_{C_0} - V_L$$

$V_{sw}$  The initial voltage across thyristor switch at the beginning of the current pulses

$V_{C_0}$  The initial voltage across  $C_0$  at the beginning of the current pulses

After the resonant current pulse reached zero, all of the thyristors are naturally turned off, and the bias current  $I_d$  begins to charge the resonant capacitor  $C_0$  linearly as  $[v_{C_0} = v_{C_0x} - (I_d \cdot t)/C_0]$  from  $(V_d - V_L + V_{sw})$  to  $(V_d - V_L - V_{sw})$  where no loss is assumed, so that the forward bias reaches the value enough to trigger the next pair of thyristors. When the forward bias has reached a settled threshold voltage, the next set of two thyristors are triggered to obtain a new current pulse.

### B. Strategy for Switching Control

The high frequency resonant switching system is cited as advantages that the input current waveform can be controlled well. Subsequently, the input power factor can be controlled and high harmonic components can be eliminated dramatically. The switching control of this system can be realized by modulating the density of current pulses to each phase. Fig. 2 shows the control block diagram of the ac-dc series resonant dc link converter using the PID operation strategy. The amplitude of input reference current  $i_{in}^*$  is decided from the required dc bias current  $I_d^*$  and the desired phase angle  $\phi$  as follows: first,  $I_d^*$  is decided by the required load voltage and load resistance ( $I_d^* = V_L/R_L$ ), then the amplitude of  $i_{in}^*$  is defined by energy balance as  $I_{in}^* = V_L I_d^* / (3V_{in} \cos \phi)$  where  $\cos \phi$  is a power factor. Further, the error signals ( $i_{ERPID}$ ) flow from the PID controller to the maximum and minimum selector circuit, then the selected signals flow to the gate driver to switch the thyristors.

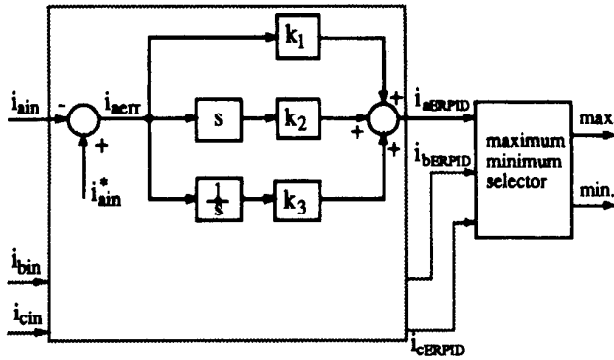


Fig. 3. PID controller block diagram.

### C. PID Operation for Input Current Control

As the error correction method in the control system, the PID operation is well-known to be simple to operate and cheap in cost. The PID operated errors ( $i_{ERPID}$ ) are generally evaluated as in the following equation for phase  $a$ ,  $b$ , and  $c$ :

$$i_{ERPID} = k_1 i_{err} + k_2 \int_0^t i_{err} dt + k_3 \frac{di_{err}}{dt} \quad (7)$$

$$i_{err} = i_{in}^* - i_{in} \quad (8)$$

where  $k_1$ ,  $k_2$ , and  $k_3$  are the coefficients of the proportional, integral and differential operations, respectively.

Fig. 3 shows the PID operation block diagram. The proportional, integral, and differential of (7), as shown in Fig. 3, is executed by using the operational amplifier. The error current ( $i_{in}^* - i_{in}$ ) is processed in proportional, integral and differential (PID) circuits.

Unlike in the PWM method, the switching for the thyristors is decided by the maximum and minimum selector circuit so as to compensate the PID-operated phase error, i.e., by comparing the error values of  $i_{ERPID}$  of each phase, the phase with maximum  $i_{ERPID}$  value, positive, and the phase with minimum  $i_{ERPID}$  value, negative, are selected as the following upper and lower switching thyristors, respectively. These  $i_{ERPID}$  signals are generated with sampling frequency as high as switching frequency. In the PID circuit, the balance of the coefficients ( $k_1$ ,  $k_2$ ,  $k_3$ ) are important; these are adjusted in accordance with load condition, etc. The adjustment was carried empirically in our study, though it can be done using the automatic tuning coefficients method [11].

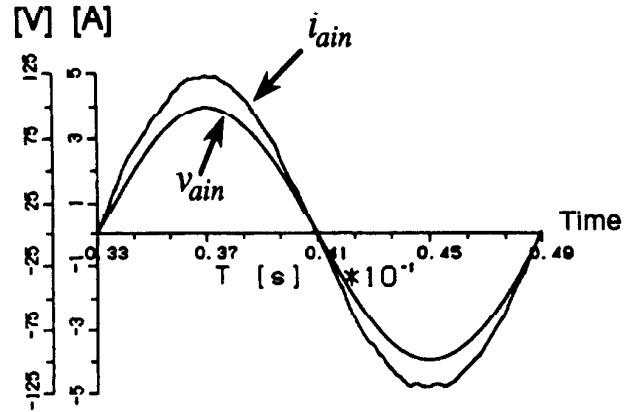
### III. SIMULATION RESULTS

The parameters of the system elements practiced in simulation are as follows: The ac input voltage is 70 [V] in phase, and the resonant elements and bias inductance are

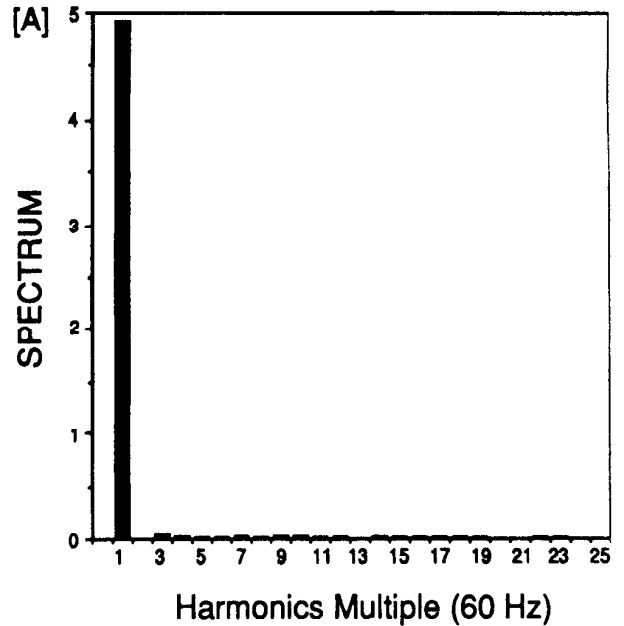
$$C_0 = 0.9 [\mu F]$$

$$L_0 = 21.4 [\mu H]$$

$$L_d = 5.0 [mH].$$



(a)



(b)

Fig. 4. (a) Simulation results of input line current  $i_{ain}$  and input phase voltage  $v_{ain}$  at expected power factor of unity. (b) Harmonic components of input line current in (a).

The filter elements are

$$L_f = 5.0 [mH]$$

$$C_f = 5.0 [\mu F].$$

The load of the system is  $R_L = 20 [\Omega]$  in parallel with  $C_L = 125 [\mu F]$ .

The simulated results of the input power factor control are depicted in Figs. 4–7. Fig. 4(a) shows the input line current  $i_{ain}$  and the input phase voltage  $v_{ain}$  waveforms, and (b) the harmonic components of input current when the power factor is expected to be unity. Fig. 5 shows  $i_{ain}$  and  $v_{ain}$  waveforms when the phase angle is  $45^\circ$  leading. Fig. 6 gives the input current and voltage waveforms when the phase angle is set

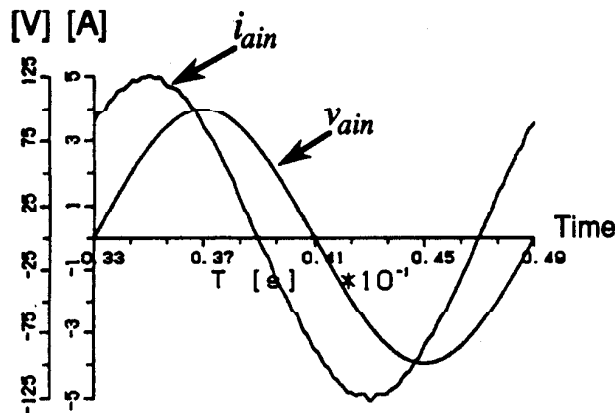


Fig. 5. Simulation results of input line current  $i_{ain}$  and input phase voltage  $v_{ain}$  at phase angle  $45^\circ$  leading.

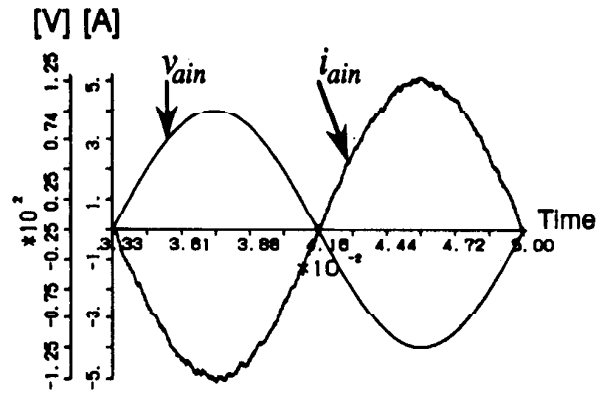


Fig. 7. Simulation results of input line current  $i_{ain}$  and input phase voltage  $v_{ain}$  at the desired power factor of  $-1$ .

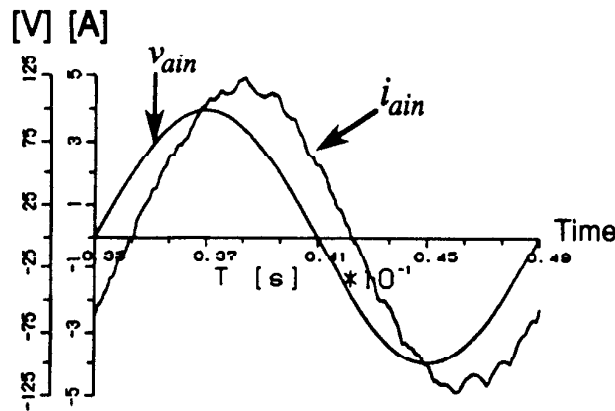


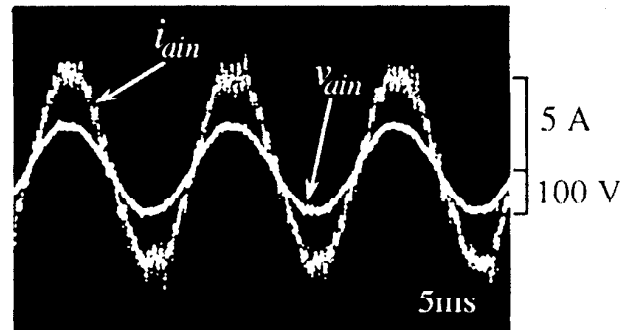
Fig. 6. Simulation results of input line current  $i_{ain}$  and input phase voltage  $v_{ain}$  set at phase angle  $30^\circ$  lagging.

$30^\circ$  lagging. Fig. 7 shows the results when the power factor of  $-1$  (regenerating mode) is desired, where  $i_{ain}$  and  $v_{ain}$  are the input current and voltage waveforms, respectively. As shown in the above simulation results, the controllable power factor and the elimination of higher harmonic components for input line current are attained by utilizing the PID operation to the system.

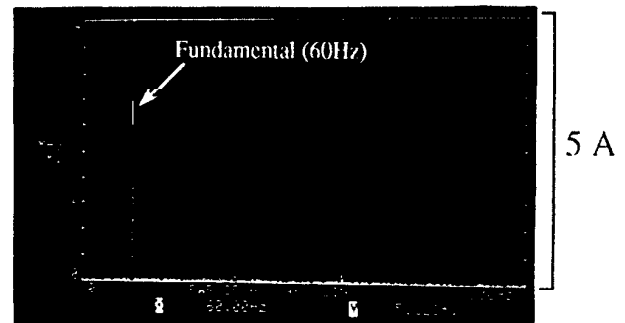
When applying the PID operation to both simulation and experiment, the tuning of the coefficients ( $k_1, k_2, k_3$ ) should be balanced. When  $k_3$  is given zero (PI circuit), the oscillation appears in the current waveform because of the resonance of the filter elements  $C_f$  and  $L_f$ . It is also clarified that when  $k_1$  is assumed large, another kind of oscillation becomes visible in the current waveform.

#### IV. EXPERIMENTAL RESULTS

The experiment of the three-phase circuit was executed with a thyristor switching control, as shown in Fig. 2. The parameters of the system are the same as in the simulation: The ac input voltage is  $70$  [V] in phase, and the resonant



(a)



(b)

Fig. 8. (a) Experimental results of input line current  $i_{ain}$  and input phase voltage  $v_{ain}$  at expected power factor of unity. (b) Harmonic components of input line current in (a).

elements and bias inductance are

$$\begin{aligned} C_0 &= 0.9 \text{ } [\mu\text{F}] \\ L_0 &= 21.4 \text{ } [\mu\text{H}] \\ L_d &= 5.0 \text{ } [\text{mH}]. \end{aligned}$$

The filter elements are

$$\begin{aligned} L_f &= 5.0 \text{ } [\text{mH}] \\ C_f &= 5.0 \text{ } [\mu\text{F}]. \end{aligned}$$

The load of the system is  $R_L = 20$  [ $\Omega$ ] in parallel with  $C_L = 125$  [ $\mu\text{F}$ ].

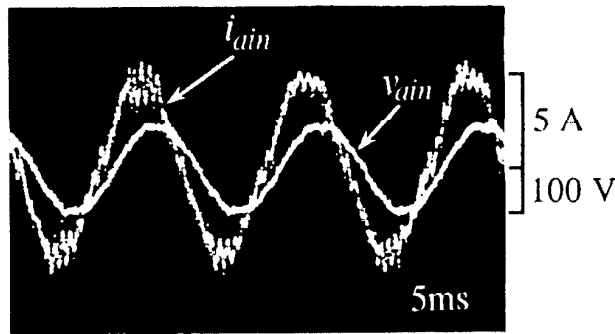


Fig. 9. Experimental results of input line current  $i_{ain}$  and input phase voltage  $v_{ain}$  at phase angle  $45^\circ$  leading.

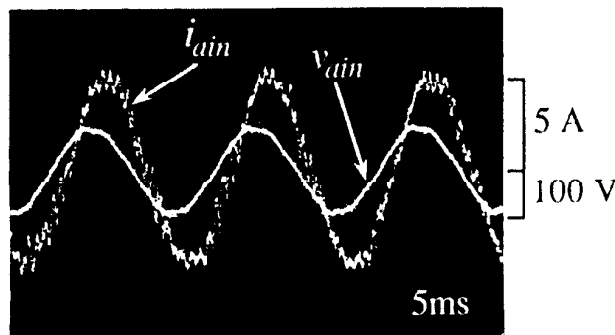


Fig. 10. Experimental results of input line current  $i_{ain}$  and input phase voltage  $v_{ain}$  set at phase angle  $30^\circ$  lagging.

In this experiment, the PID operation strategy was implemented to realize the input current controller, i.e., the controllable power factor. The switching frequency as high as 20 kHz was utilized in our experiment.

The experimental results of this system are given in Figs. 8–12. Fig. 8(a) shows the input line current  $i_{ain}$ , the input phase voltage  $v_{ain}$  waveforms, and (b) the harmonics components of input current when the power factor is expected to be unity. Fig. 9 shows  $i_{ain}$  and  $v_{ain}$  waveforms when the phase angle is  $45^\circ$  leading. Fig. 10 shows the current and the voltage waveforms when the phase angle is set  $30^\circ$  lagging. Fig. 11 is the single phase circuit to realize power factor  $-1$  (regenerative), and Fig. 12 shows the resulting waveforms of  $i_{ain}$  and  $v_{ain}$ . In those experiments, the power factor can be controlled well in desired value, and the current waveforms include low harmonic components.

In comparison with the current waveform of the conventional PWM control method [2], the amount of higher harmonics seems to be small in the experiment. This method has the features of low EMI (electro magnetic interference) and low switching losses because of utilizing high frequency resonant switching.

## V. CONCLUSION

The three-phase ac-dc series resonant dc link converter using the PID operation is proposed to realize the power converter system with controllable power factor. The method of input power factor control using PID operation is discussed

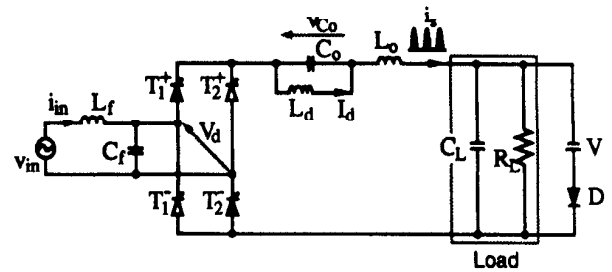


Fig. 11. Single phase circuit for power factor of  $-1$ .

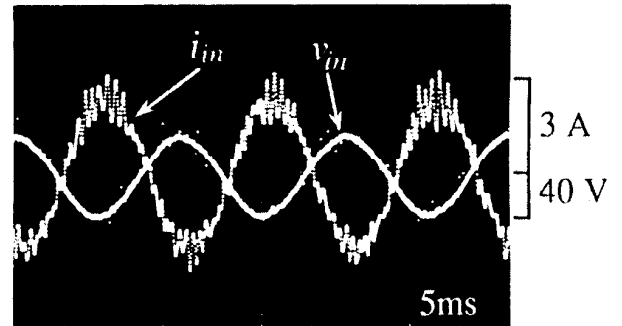


Fig. 12. Experimental results of input current  $i_{in}$  and input phase voltage  $v_{in}$  of single phase circuit at the desired power factor of  $-1$ .

in the simulation and verified in the experiment. By utilizing the PID operation strategy, the input power factor can be controlled in unity or desired value and the elimination of higher harmonic components can be attained well

## REFERENCES

- [1] S. Manias and P. D. Ziogas, "A novel sinewave in ac to dc converter with high frequency transformer isolation," *IEEE Trans. Ind. Electron.*, vol. IE-32, no. 4, pp. 430–438, Nov. 1985.
- [2] K. Inagaki, T. Furuhashi, A. Ishiguro, M. Ishida, and S. Okuma, "A new PWM control for ac to dc converters with high frequency transformer isolation," *IEEE Trans. Ind. Applicat.*, vol. 29, no. 3, pp. 486–492, May/June 1985.
- [3] R. Wu, S. B. Dewan, and G. R. Slemon, "A PWM ac to dc converter with fixed switching frequency," in *IEEE-IAS Ann. Meet. Conf. Rec.*, 1988, pp. 706–711.
- [4] Y. Murai and T. A. Lipo, "High frequency series resonant dc link power conversion," *IEEE Trans. Ind. Applicat.*, vol. IA-28, no. 6, pp. 1277–1285, Nov./Dec. 1992.
- [5] D. M. Divan, "The resonant dc link converter—A new concept in static power conversion," *IEEE Trans. Ind. Applicat.*, vol. 25, no. 2, pp. 317–325, Mar./Apr. 1989.
- [6] P. Sood and T. A. Lipo, "Power conversion system using a resonant high frequency ac link," in *IEEE-IAS Ann. Meet. Conf. Rec.*, 1986, pp. 333–341.
- [7] P. Caldeira, K. W. Marschke, M. T. Aydemir, T. A. Lipo, and Y. Murai, "Utilization of the series resonant dc link as a dc motor drive," in *IEEE-IAS Ann. Meet. Conf. Rec.*, 1990, pp. 813–819.
- [8] M. Yoshida, H. Soebagia, Y. Murai, and T. A. Lipo, "Series resonant dc link dual converter as a dc motor drive," in *EPE '93-Brighton Annu. Meet. Conf. Rec.*, 1993, vol. 5, pp. 188–193.
- [9] H. Soebagia, M. Yoshida, Y. Murai, and T. A. Lipo, "A comparative study of input power converter switching between phase control method and series resonant dc link method," in *IEE-Japan IAS Conf. Rec.* (in Japanese), 1993, pp. 315–320.
- [10] F. R. Burgseth and S. S. Venkata, *Electric Energy Devices*. Englewood Cliffs, NJ: Prentice-Hall, 1987, p. 329.
- [11] Takeshi Mori *et al.*, "PID auto tuning controller," *Trans. Design Control*, vol. 29-8, pp. 723–728, 1990 (in Japanese).